GA–A27415

OBSERVATION OF LOCALIZED FAST-ION HEAT LOADS IN TEST BLANKET MODULE SIMULATION EXPERIMENTS ON DIII-D

by

G.J. KRAMER, A.G. McLEAN, N.H. BROOKS, R.V. BUDNY, R. ELLIS, W.W. HEIDBRINK, T. KURKI-SUONIO, R. NAZIKIAN, T. KOSKELA, M.J. SCHAFFER, K. SHINOHARA, J.A. SNIPES, D.A. SPONG, and M.A. VAN ZEELAND

OCTOBER 2012

GENERAL ATOMICS

GA–A27415

OBSERVATION OF LOCALIZED FAST-ION HEAT LOADS IN TEST BLANKET MODULE SIMULATION EXPERIMENTS ON DIII-D

by

G.J. KRAMER,* A.G. McLEAN,† N.H. BROOKS, R.V. BUDNY,* R. ELLIS,*
W.W. HEIDBRINK,‡ T. KURKI-SUONIO,# R. NAZIKIAN,* T. KOSKELA,# M.J. SCHAFFER,
K. SHINOHARA,¶ J.A. SNIPES,§ D.A. SPONG,◊ and M.A. VAN ZEELAND

This is a preprint of a paper to be presented at the Twenty-fourth IAEA Fusion Energy Conf., October 8-13, 2012 in San Diego, California.

*Princeton Plasma Physics Laboratory, Princeton, New Jersey.
†Lawrence Livermore National Laboratory, Livermore, California.
‡University of California Irvine, Irvine, California.
#Helsinki Universiy of Technology, Helsinki, Finland.
¶Japan Atomic Energy Agency, Naka, Japan.
§ITER Organization, Cadarache, France.
◊Oak Ridge National Laboratory, Oak Ridge, Tennessee.

Work supported in part by
the U.S. Department of Energy
under DE-AC02-09CH11466, DE-AC52-07NA27344, DE-FC02-04ER54698, SC-G904302, and DE-AC05-00OR22725

GENERAL ATOMICS PROJECT 30200
OCTOBER 2012

Observation of Localized Fast-Ion Heat Loads in Test Blanket Module Simulation Experiments on DIII-D

G.J. Kramer 1), A.G. McLean 2), N.H. Brooks 3), R.V. Budny 1), R. Ellis 1), W.W. Heidbrink 4), T. Kurki-Suonio 5), R. Nazikian 1), T. Koskela 5), M.J. Schaffer 3), K. Sinohara 6), J.A. Snipes 7), D.A. Spong 8), and M.A. Van Zeeland 3)

1) Princeton Plasma Physics Laboratory, PO Box 451, Princeton, NJ 08543-0451, USA.
2) Lawrence Livermore National Laboratory, Livermore, CA 94550, USA
3) General Atomics, PO Box 85608, San Diego, CA 92186-5608, USA.
4) University of California Irvine, Irvine, CA 92697, USA.
5) Helsinki University of Technology, Helsinki, Finland.
6) Japan Atomic Energy Agency, 801-1 Mukouyama, Naka City, Ibaraki, 311-0193, Japan.
7) ITER Organization, Route de Vinon sur Verdon, 13115 St. Paul lez Durance, France
8) Oak Ridge National Laboratory, PO Box 2008, Oak Ridge, TN 37831, USA.

e-mail contact of main author: gkramer@pppl.gov

Abstract. Infrared imaging of hot spots induced by localized magnetic perturbations using the Test Blanket Module (TBM) mock-up on DIII-D is compared with beam-ion loss simulations. The hot spots were seen on the carbon protective tiles surrounding the TBM as they reached temperatures over 1000°C. Both the localization and peak intensity of the hot spots are in fair agreement with fast-ion loss simulations using a range of codes: ASCOT, SPIRAL, and OFMC. The orbit calculations take into account the birth profile of the beam ions as well as the scattering and slowing down of the ions as they interact with the localized TBM field. The close agreement between orbit calculations and measurements validate the analysis of beam ion loss calculations for ITER where ferritic material inside the tritium breeding TBMs is expected to produce localized hot spots on the first wall.

1. Introduction

A major goal on ITER is to study tritium breeding in test blanket modules. Six Test Blanket Modules (TBMs), two in each of three equatorial ports, are being envisioned for ITER. These TBMs contain a significant amount of ferritic steel, and therefore, the TBMs will create three highly localized distortions of the magnetic field which can reduce the confinement of fast ions, especially the fusion-born alpha particles. In alpha-particle confinement simulations for ITER it was shown that a substantial fraction of the lost alpha particles is deposited on the surface of the TBMs thereby creating hot spots [1, 2, 3].

During TBM experiments in DIII-D [4] in which a scaled mock-up of a TBM equatorial port for ITER was placed in the machine, the confinement of fast beam-ions was studied. The mock-up TBM on DIII-D has four protective carbon tiles arranged vertically with a thermocouple placed on the back of each 2.5 cm thick tile (Fig. 1).

In a first series of experiments (in 2009) the thermocouple signals were used to deduce fast-ion induced heat loads on the surface of the tiles [3]. This involved modeling of the fast-ion losses to the TBM tiles in the presence of a highly localized error field near the TBM mock-up (Fig. 1) and the modeling of the heat transport through the tiles.

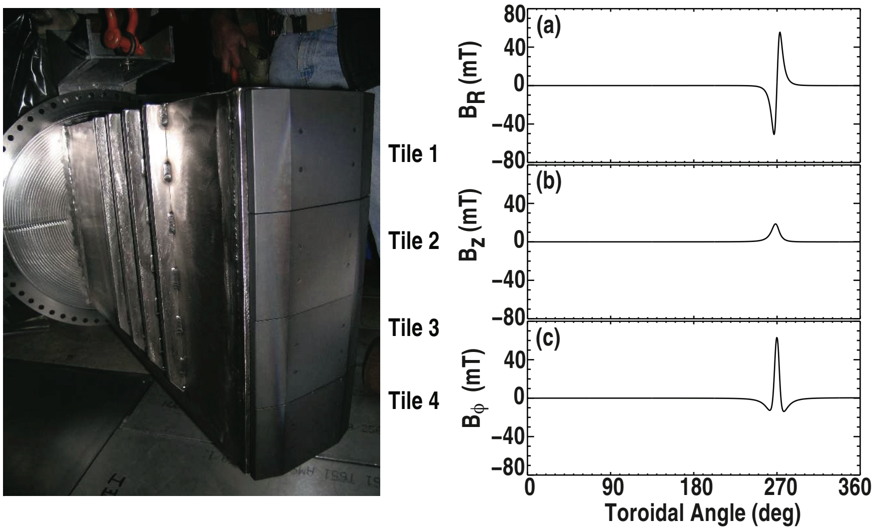

FIG. 1. The four protective carbon tiles on the DIII D TBM mock-up assembly (left). The (a) radial, (b) vertical, and (c) toroidal magnetic field components generated by the TBM mock-up in DIII-D on the midplane at the low-field side plasma edge.

Although good agreement between the measured and modeled thermocouple temperature response was found, there were still questions about possible heat load contributions from the thermal plasma and of the precise shape of the hot spot on the tiles. In those studies four fast-ion transport codes were used, the ASCOT code [5], the DELTA5D Monte Carlo code [6], the OFMC code [7, 8] and the SPIRAL code [1]. The codes gave very similar answers for the total power deposited in the TBM hot spots but the details on the size, shape, and peak heat loads of the spot were different. Those differences in the fast-ion loss simulations can only be resolved by measuring the hot spot on the tiles directly with an Infra Red (IR) thermal imaging camera. In this paper the results of IR imaging experiments which were performed last year are reported.

First, the alternate explanation for the heat loads, thermal plasma moving close enough to the tiles when the TBM fields are engaged and so contributing to the thermal heat load, is investigated and ruled out based on the thermal images (Sec. 2). Once it was established that the heat loads were completely due to TBM-induced beam-ion losses, we have injected the various beams in DIII-D separately to measure the TBM hot spot for different pitch angle distributions (Sec. 2). Those pitch-angle resolved losses are compared with results from three fast-ion loss simulation codes (ASCOT, OFMC, and SPIRAL) that can propagate the particles to the DIII-D wall (Sec. 3). From a favorable comparison between the experiments and simulations it is concluded that the fast-ion loss codes can be used with some caution to estimate heat loads on the TBM surfaces in ITER (Sec. 4).

2. Experiments

In three similar discharges with toroidal magnetic field 1.7 T, plasma current 1.2 MA, ELMy H-mode plasma with central density 3.7×10^{19} m^{-3}, electron temperature 2.7 keV, gap between last closed flux surface and the TBM tiles 4.4 cm, the thermal plasma contribution to the tile heating was investigated. In the first discharge 2 MW of Neutral Beam Injection (NBI) was used without TBM fields. No heating of the TBM tiles was observed with the IR camera as can be seen in Fig. 2(a). In the second discharge the TBM fields were engaged during the 2 MW NBI heating phase. This resulted in a significant heating of the tiles [Fig. 2(b)]. In the third discharge the NBI was replaced by 3.3 MW of Electron Cyclotron Heating (ECH) while the TBM fields were engaged. No significant heating of the TBM tiles was observed as can be seen in Fig. 2(c).

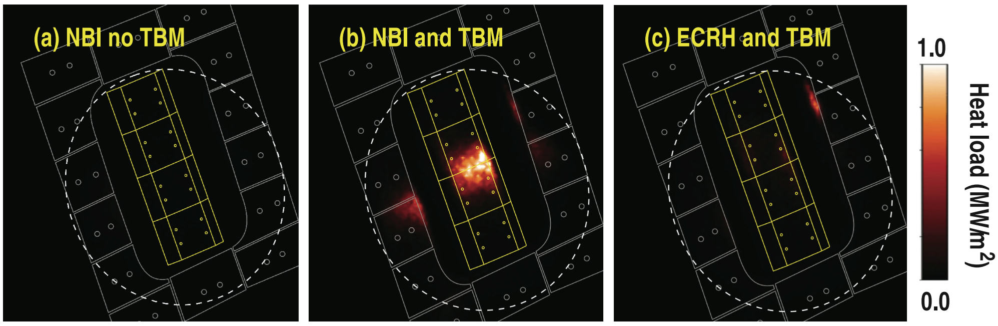

FIG. 2. Heat loads in similar discharges: (a) 2 MW of NBI without TBM fields, (b) 2 MW of NBI with TBM fields, and (c) 3.3 MW electron cyclotron resonance heating (ECRH) with TBM fields showing that only the combination of TBM fields and fast ions from NBI injection creates a hot spot on the TBM tiles..

These experiments demonstrate that beam-ions in combination with the TBM fields produce the observed hot spots on the TBM protective tiles in DIII-D and not the interaction between thermal plasma and the TBM tiles when the TBM fields are present. Those experiments confirm the interpretation given in [3] of the TBM tile temperature rise as caused by fast-ion losses to the protective TBM tiles.

We can utilize the TBM error fields in combination with NBI from various beam lines, shown in Fig. 3, as a sensitive tool to benchmark fast-ion loss simulation codes by comparing the simulated heat loads with measured ones from the IR imaging. Particles from different beams have characteristic pitch distributions (Fig. 3) whereby the pitch is defined as $v_{\|}/v$ with v the particle velocity and $v_{\|}$ parallel to the magnetic field line whereby a positive sign is defined in the direction of the plasma current. By injecting the beams separately pitch dependence of the TBM induced losses was obtained.

During a DIII-D discharge (shot #147603) which was very similar to the discharges used in the fast-ion heating studies, the TBM coils were engaged for 2 s during the stationary flat top phase of the discharge while the 030L beam was injected at half power to keep the plasma in H-mode, the other beams were injected one by one for 180 ms in 350 ms periods. During each 180 ms injection period a full slowing-down distribution is created (the fast-ion energy slowing-down time is about 60 ms) followed by a period where the slowing-down distribution thermalizes. In this way the heat loads from successive beams on the TBM tiles was measured in a single discharge.

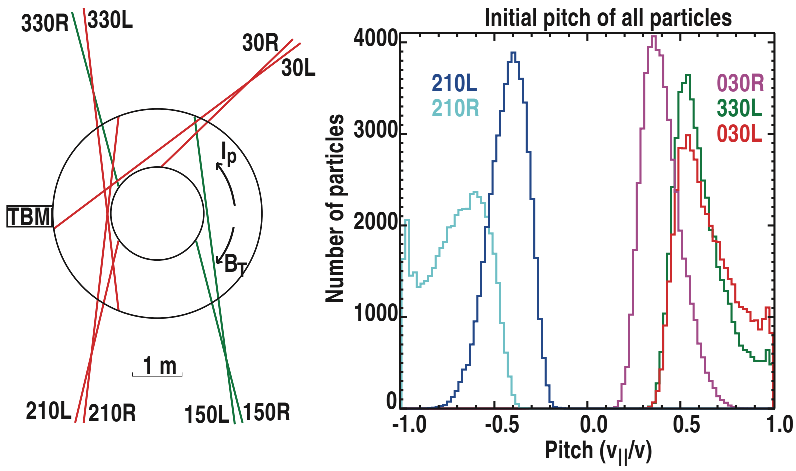

FIG. 3. The layout of the various beams in DIII-D. Beam lines in red were used in the current experiments. The pitch distribution created by the various beam lines.

Heat loads on the TBM tiles were obtained from the measured IR temperature data by using the THEODOR 2-D analysis code [9]. The thermal analysis included temperature dependent heat diffusion and conduction coefficients for the AJT graphite while a loosely adhered surface layer was taken into account with a heat transmission coefficient of 5 MW/m^2/K. In the heat load analysis care was taken not to include the increased heat loads due to ELMs. The power that was deposited onto the TBM surface was obtained by integrating the heat load over all the four tiles and is given in the second column of Table 1 while the measured heat loads are shown in the left-hand side column of Fig. 4.

Table 1. *The power deposited in the hot spot on the TBM tiles in the experiment and as calculated by the ASCOT, OFMC, and SPIRAL codes. Typical uncertainties in the experimental values are 30%.*

	PowerDepositedonTBMTiles(kW)			
DIII-D Beam	Experiment	ASCOT	OFMC	SPIRAL
030R + 0.5 030L	90.2	50.7	66.5	44.9
210L + 0.5 030L	107.7	44.1	72.7	71.9
0.5 030L	48.1	13.1	13.6	14.8
210R + 0.5 030L	92.0	56.5	46.5	39.6
330L + 0.5 030L	59.3	56.1	45.5	33.2

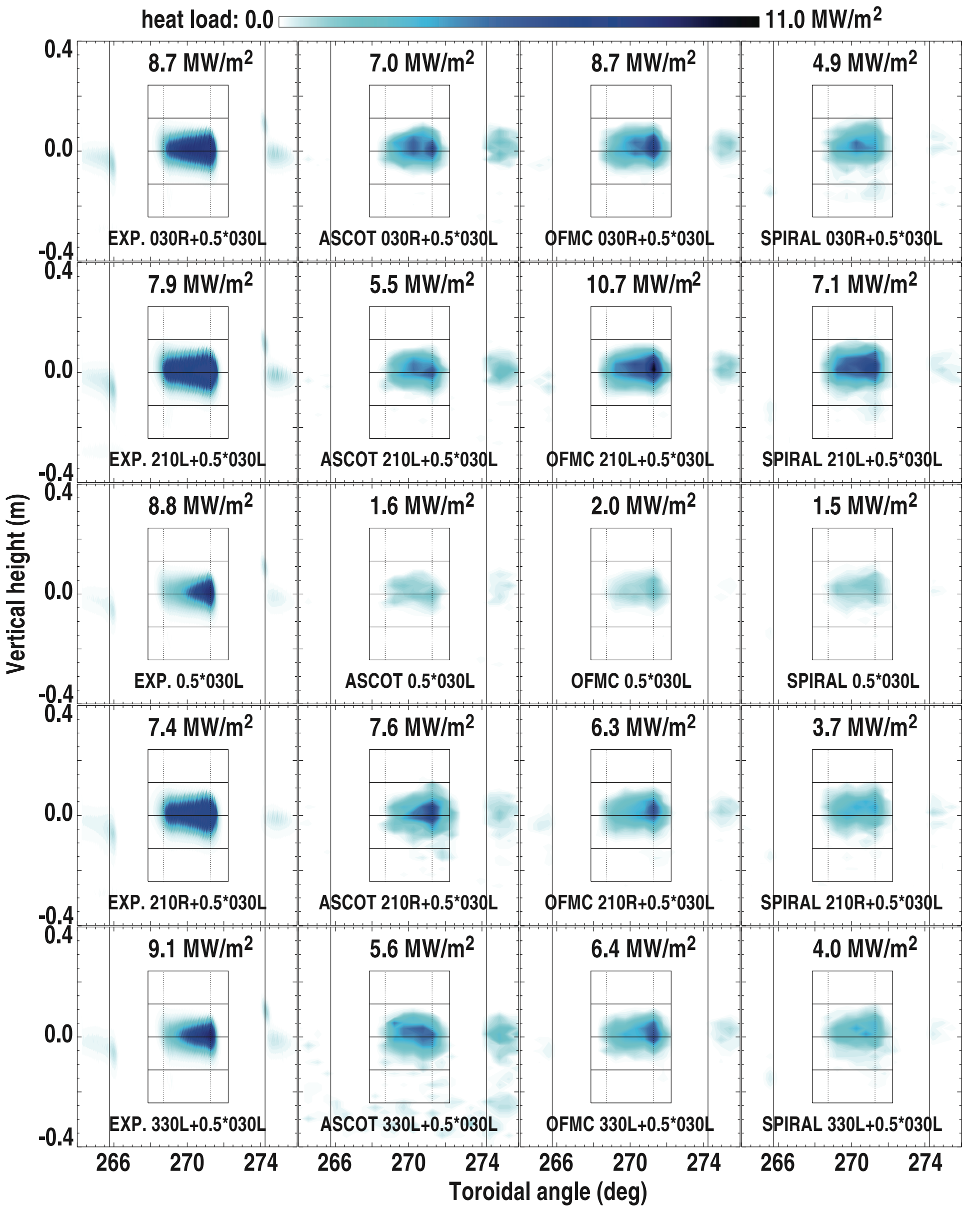

FIG. 4. Measured heat loads (left column) compared to heat loads as calculated with the ASCOT (second), OFMC (third), and SPIRAL (last column) codes for the five beams. For each frame the peak heat load is given.

The total power that is deposited by the perpendicular counter-going beam (210L) is almost 20% higher than the equivalent co-going beam (030R). The same holds for the parallel beams (co-going: 330L, counter-going: 210R), with an increase in measured heat load from co to counter deposition of 55%. The power deposition from the half co-going beam (030L) is rather puzzling. The expectation was, based on the fast-ion loss simulations as discussed later, that this beam would only give a low power deposition on the tiles but when this beam is injected alone it delivers 48 kW on the TBM tiles while injected together with the parallel 330L beam the power deposition increases only by 11.2 kW.

3. Particle-Loss and Heat-Load Simulations

Beam-ion transport was calculated with three different codes: the OFMC code which is guiding-center following code and the ASCOT and SPIRAL codes which are full-orbit following codes. All three codes use an axisymmetric EFIT equilibrium [10] with the full 3-D vacuum ripple field induced by the TBM superimposed on it. All three codes solve for the trajectory of birth energy beam ions (with initial energies varying between 75 and 80 keV depending on the used NBI source) and using the actual toroidally asymmetric beam deposition profiles as calculated by TRANSP/NUBEAM [11]. This removes the uncertainty on the birth profiles when the results from the different codes are compared. Three of the five beams were injected in the co-current direction (030L, 030R, and 330L) while the other two (210L, and 210R) were injected in the counter-current direction resulting in anisotropic pitch distributions as shown in Fig. 3. The particles were followed beyond the separatrix to a outer cylinder in DIII-D at 2.377 m. In all three codes the three poloidal limiters at 95, 230, and 310 deg. were included together with an accurate model of the TBM tiles that included the beveled tile shape and the space of the port next to the tiles.

Slowing down and collisions [12] were included in all the codes and particles were followed until they reached thermal velocities or got lost to the wall.

All three codes show the formation of a hot spot on the central two TBM tiles as shown in Fig. 4 which is in agreement with the measurements. The total power deposited in the hot spot on the TBM tiles varies somewhat between the different codes. OFMC and SPIRAL show the highest power deposited for the counter-going perpendicular beam (210L) while ASCOT predicts significant lower losses from that beam. Both OFMC and SPIRAL show enhanced losses from the counter-going perpendicular beam (210L) compared to the co-going perpendicular beam (030R) which can be explained by enhanced prompt losses due to the counter-injection. ASCOT does not find those enhanced counter-injection losses for the perpendicular beams. All three codes agree well on the power that is deposited by the continuous half beam (a beam injected at full power with a 50% duty cycle) (030L). ASCOT and OFMC both find that the deposited power for the co and counter tangential beams (330L and 210R) are the same although OFMC predicts less power than ASCOT while SPIRAL finds about 20% more losses from the counter injected tangential beam (210R) compared to the co-injected tangential beam (330L). The power deposited on the TBM tiles from tangential injection from SPIRAL is less than the power deposited as calculated by ASCOT and OFMC.

All three codes predict slightly different hot-spot foot prints on the TBM tiles as can be seen in Fig. 4. In combination with the difference in deposited power, it is not surprising to find variations in the peak heat loads as listed in Fig. 4. In most cases OFMC gives the highest heat load which occurs at the transition between flat surface and the beveled edge that faces the plasma current. For the co- and counter perpendicular beams (030R and 210L) both OFMC and SPIRAL find the highest heat loads for the counter injected beam (210L) while ASCOT finds the opposite. Heat loads from the co- and counter tangential beams (330L and 210R) are found to be similar for OFMC and ASCOT while the SPIRAL heat loads are lower than the ASCOT and OFMC results.

All the codes underestimate the measured power deposition on the TBM tiles. This might be due to plasma effects such as turbulence and low levels of MHD activity and/or due to the sensitivity of the power deposition to the gap between last-closed surface and the tiles as was found in [3]. Increased heat loads due to ELMS, were omitted from the reported experimental results. In the simulations only the effects of the TBM error fields were included but the fast-ion transport can be enhanced by turbulence and MHD activity. However, the discharges were selected for their low MHD activity. The simulated foot prints of the hot spots compare in general well with the measured foot prints (Fig. 4) although the simulated foot prints are more fuzzy at the edges due to the limited statistics in the simulations. The simulated peak heat loads are in some cases in agreement with the measurements (ASCOT: 030L, 210R; OFMC: 030L; SPIRAL: 210L), in one case it is overestimated (OFMC: 210L) while in most cases (ASCOT: 210L, 030L, 330L; OFMC: 030L, 210R, 330L; SPIRAL: 030R, 030L, 210R, 330L) the measured heat loads are underestimated. The inclusion of plasma effects (MHD activity, and edge turbulence) in the simulations and a slightly smaller gap might increase the simulated heat loads and power deposited onto the TBM tiles bringing the simulations closer to the experimental values.

4. Discussion and Conclusion

Thermal imaging experiments of the protective TBM tiles in DIII-D have shown that the magnetic fields generated by a scaled mock-up of a TBM equatorial port for ITER create a hot spot on the two central carbon tiles that protect the TBM surface during NBI. It was shown that this hot spot only appears with the TBM fields present during NBI and therefore, it was concluded that the hot spot is due to fast-ion losses. In a systematic scan of the different beam lines in DIII-D which corresponds to varying the fast-ion pitch distribution, heat loads of up to 9 $\mathrm{MW/m^2}$ were found and more than 100 kW was deposited in the hot spot when 2.4 MW of counter perpendicular NBI was injected. An anomalous high heat load was found when a single 1.1 MW parallel beam was injected which is not yet understood from fast-ion loss simulations and the subject of further study.

Beam-ion loss calculations with different fast-particle orbit-following codes confirmed that the observed heating of the two central tiles is caused by beam-ion losses. The size and shape of the calculated hot spots agreed well for all three codes. The total power deposited on the tiles was underestimated in the simulations. However, the deposited power depends very sensitively on the gap width, and enhanced fast-ion transport due to MHD activity and plasma turbulence were neglected. Simulated heat loads are in general within 30% of the observed ones, giving confidence in using the fast-ion transport codes for estimating heat loads on the TBM modules in ITER.

This work was supported by the US Department of Energy under DE-AC02-09CH11466, SC-G903402, DE-FC02-04ER54698 and DE-AC05-00OR22725. The supercomputing resources of CSC - IT center for science were utilized in the studies. This work was partially funded by the Academy of Finland projects No. 121371 and 134924. The views and opinions expressed herein do not necessarily reflect those of the ITER Organization.

References

[1] KRAMER, G.J., et al., Fusion Energy Conference 2008 (Proc. 22nd Int. Conf. Geneva, 2008) CD-ROM file IT/P6-3 and KRAMER, G.J., et al., “A description of the full particle orbit following SPIRAL code for simulating fast-ion experiments in Tokamaks,” submitted to Plasma Physics and Controlled Fusion (2012).
[2] KURKI-SUONIO, T., et al., Nucl. Fusion **49** (2009) 095001
[3] KRAMER, G.J., et al. Nucl. Fusion **51** (2011) 103029
[4] SCHAFFER, M.J., et al., Nucl. Fusion **51** (2011) 103028
[5] HEIKKINEN, J.A. and Sipilä, S.K., Phys. Plasmas **2** (1995) 3724
[6] SPONG, D.A., Phys. Plasmas **18** (2011) 056109
[7] TANI, K., et al., J. Phys. Soc. Jpn **50** (1981) 1726
[8] SHINOHARA, K., et. al., Nucl. Fusion **43** (2003) 586
[9] HERRMANN, A., Plasma Phys. and Controlled Fusion **44** (2002) 883
[10] LAO, L.L., et al., Nucl. Fusion **30** (1990) 1035
[11] BUDNY, R.V., et al., Nucl. Fusion **35** (1995) 1497
[12] BOOZER, A.H. and KUO-PETRAVIC, G., Phys. Fluids **24** (1981) 851 (1981).